Design of a Lab-On-Chip Cartridge for the Optical Detection of Small Molecules based on Dye-Displacement MIPs

Design of a Lab-on-Chip Cartridge for the Optical Detection of Small Molecules Based on Dye-Displacement MIPs

Juul Goossens, Thijs Vandenryt, Joseph W. Lowdon, Bart van Grinsven, Kasper Eersels, Wim Deferme, and Ronald Thoelen

***Abstract*— Molecular imprinted polymers (MIPs) are well known for their specific recognition of a wide variety of different analytes. However, the complex immobilization process of MIPs onto sensor electrodes poses a significant challenge. This research introduces a novel approach to enhance the application potential of MIPs by exploiting dye-displacement MIPs. These synthetic receptors can selectively release dye upon exposure to an aqueous target. A disposable and low-cost lab-on-chip cartridge is presented, enabling the MIPs to interact with the target solution for dye displacement. Furthermore, these cartridges are coupled to a portable optical sensor setup that can be used for screening samples in a user-friendly and fast manner. Characterization experiments demonstrate the capability of the spectrometer setup to identify different color dyes and intensities. Finally, a proof-of-application shows the use of our sensing setup for the indirect detection of 2-methoxphenidine (2-MXP) using dye-loaded MIPs, employing a dose–response characterization (4PL). Furthermore, as the dye displacement and sensing principle are universal, this setup holds promise for various other sensing applications, including food quality assessment, environmental testing, and pharmaceutical analysis.**

***Index Terms*— Dye–displacement molecular imprinted polymer (MIP), integrated lab-on-chip cartridge, portable spectrometer.**

I. Introduction

MOLECULAR imprinted polymers (MIPs) have shown great scientific developments in the last decades. These synthetic polymer receptors are attractive not only for their specific recognition of a wide variety of different analytes, but also for their superior chemical and physical stability over natural receptors. These characteristics make MIPs a very attractive type of receptor to be used for sensing applications [1], [2], [3], [4].

Manuscript received 13 March 2023; revised 26 June 2023; accepted 19 July 2023. Date of publication 2 August 2023; date of current version 16 August 2023. This work was supported by the European Union's Regional Development Fund through the Interreg Va Euregion Meuse Rhine (EMR) Project Food Screening. The Associate Editor coordinating the review process was Dr. Yunjie Yang. *(Corresponding author: Juul Goossens.)*

Juul Goossens, Thijs Vandenryt, Wim Deferme, and Ronald Thoelen are with the Institute for Materials Research (IMO), Hasselt University, 3590 Diepenbeek, Belgium, and also with IMEC vzw, Division IMOMEC, 3590 Diepenbeek, Belgium (e-mail: juul.goossens@uhasselt.be; thijs.vandenryt@uhasselt.be; wim.deferme@uhasselt.be; ronald.thoelen@uhasselt.be).

Joseph W. Lowdon, Bart van Grinsven, and Kasper Eersels are with the Maastricht Science Program, Maastricht University, 6200 Maastricht, The Netherlands (e-mail: joe.lowdon@maastrichtuniversity.nl; bart.vangrinsven@maastrichtuniversity.nl; kasper.eersels@maastrichtuniversity.nl).

Digital Object Identifier 10.1109/TIM.2023.3301040

The most frequently used technique for the fabrication of MIPs is monolithic bulk polymerization. Despite being highly popular, the formed bulk polymer has to be crushed, ground, and sieved before use which results in a particle powder with varying sizes and shapes [5], [6]. This makes attaching the bulk MIP powder to a sensor interface challenging and difficult to reproduce [7], [8]. This is one of the main bottlenecks toward the commercialization of MIP-based sensors. However, when MIPs are employed in an indirect colorimetric assay, a process where a change in color can indicate the presence of the target, it can overcome the challenge of coupling MIPs to a sensor interface [8], [9]. Loading a dye inside the MIP-cavities and performing a dye displacement assay, in which the dye is displaced through competitive binding with the template, is a fairly straightforward approach to indirectly detect chemical targets in solution [10]. Upon binding, the MIPs can be filtered from the solution, and the absorption of the filtrate can be measured at the fingerprint wavelength corresponding to the dye. The more target is present in the solution, the stronger the color effect in the filtrate [11], [12].

Despite this prominent advantage of the MIP dye-displacement assay, the sensor application potential is yet unexplored. Currently, these MIPs are only being tested in laboratory settings for development research purposes. The colorimetric testing is done by equilibrating the analyte and the dye-loaded MIP, while the readout is happening via expensive lab-grade benchtop spectrometer equipment [9], [12], [13], [14]. This process is too expensive and labor-intensive for high-throughput screening purposes. However, MIPs are potentially very good candidates for lab-on-chip applications if they can be implemented into cheap, disposable samplers coupled to low-cost, portable read-out systems [3], [9].

Optical spectroscopy is a very good method to achieve such a readout technology and is therefore a widespread and very powerful tool in research. It has the advantage of being nondestructive with a fast response time [15], [16]. However, commercial spectroscopy units are typically expensive, bulky devices, that are operated by trained personnel as they offer high degrees of sensitivity and full coverage of the entire electromagnetic spectrum [16], [17], [18]. Yet, dye-displacement assays only need analysis at particular wavelengths and do not require high-end resolution. Therefore, low-cost and portable measuring setup can prove extremely useful, especially in

day-to-day measurements, where convenience outweighs the need for lab-grade precision [18], [19]. Previous research already demonstrated the use of spectrometer-on-chip portable sensing systems in biosensor research. For instance, they have been employed in detecting vitamin B12 [19] and vitamin A [20]. Besides, different approaches based on diffraction grating and the use of multiple LEDs have proven effective for the detection of plasma glucose [21] and mercuric ions [22]. The use of smartphone-based analysis systems is also on the rise due to their high portability and widespread availability [23]. However, it is important to note that these developed systems primarily focus on the development of the sensing platform rather than the application itself. Consequently, they are based on a cuvette format. Nevertheless, is it important to recognize the integration of the application. An extremely high sensitivity is required to measure the spectral absorbance of small volumes in microfluidic devices [24]. Consequently, research has focused on developing absorption spectroscopy sensing systems that facilitate the measurement of small volumes. For example, the use of a multireflection flow cell for the analysis of reactive phosphorus [25] and the detection of urea and glucose by harnessing the emission band of short-wave infrared LEDs [26].

This research aims to demonstrate the integration of an MIP dye displacement into a disposable lab-on-chip cartridge in combination with a spectrometer-on-chip for quick and accurate analyte testing. The goal is to develop a sensing system that can be used for on-site or at-line analysis with a focus on portability, ease of use, cost, and disposability. A lab-on-chip cartridge is presented wherein dye-displacement MIPs are incorporated. Upon binding the target to the MIP, a dye is released that will be transported to a readout compartment that is aligned with a spectrophotometer. The application demonstrated in this study is the specific detection of 2-methoxphenidine (2-MXP) [11], a designer drug [27], [28], [29]. However, as the dye displacement and sensing principle are universal, this principle could also be extended toward the detection of other small molecules for various other applications like assessing food quality, environmental testing, pharmaceutical testing, and so on. The sensor presented in this study could bridge the gap between academic MIP technology, which has mostly been confined to laboratory settings, and its commercial potential. To illustrate the potential of the setup, the capability of the mini-spectrometer to detect different dye molecules at various intensities is tested. Afterward, a lab-on-chip cartridge is used to perform the dye displacement-based detection of 2-MXP.

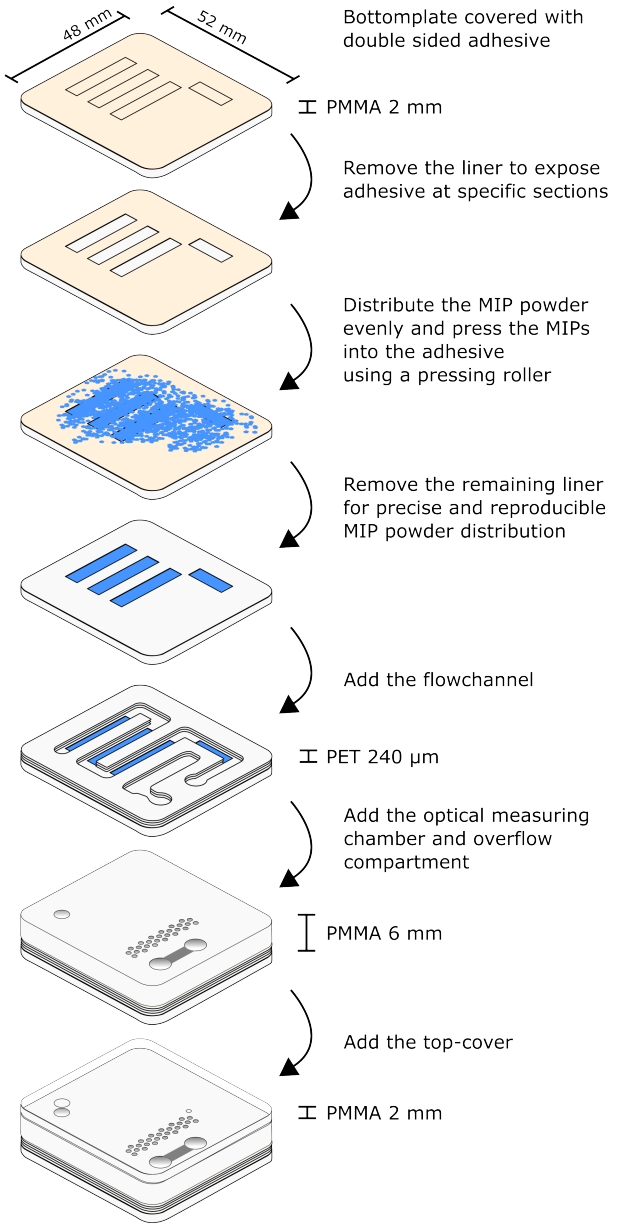

Fig. 1. MIP powder immobilization and cartridge assembly process. The assembly of the cartridge is pictured step-by-step. Different materials and geometric specifications are given. All different layers are stacked together via double-sided adhesives (not shown in schematic).

II. Materials and Methods

A. Lab-on-Chip Cartridge Design

The lab-on-chip cartridge is designed in such a manner that ensures the sample handling, performs the dye-displacement assay, and holds the displaced dye in a measurement compartment for analysis. Bulk MIPs are incorporated into the developed cartridge by immobilization inside a flow channel. The cartridge assembly is demonstrated in Fig. 1. The process starts with a 2-mm PMMA (poly(methyl methacrylate), Kunststofshop, The Netherlands) sheet covered with double-sided adhesive (7955MP, 3M, United States). The adhesive liner is removed at specific sections for easy and reproducible MIP powder distribution. After the exposed adhesive sections are fully covered with MIP powder, the particles are pressed onto the adhesive by the use of a pressing roller (Silicone, Iguna, The Netherlands); the excess, nonadherent, powder was removed afterward. This process ensures that the amount of MIPs is dependent on the surface area rather than weight. Then, the remaining adhesive liner is removed altogether which results in precise and reproducible MIP-covered adhesive sections. Afterward, a PET flow channel (240-μm thick; polyethylene terephthalate, Pavo, The Netherlands) is placed on top. The MIP-covered sections

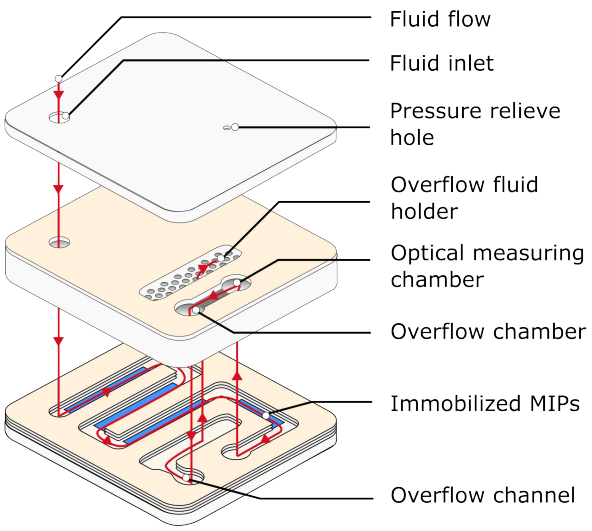

Fig. 2. Exploded view of the lab-on-chip cartridge. All different parts of the cartridge are shown. The red arrow indicates the fluid flow in the final assembled system.

are now lined up with the straight sections of the flow channel. At last, a 6-mm-thick PMMA sheet, which holds the optical measuring chamber and the overflow compartment, is added. Finally, a 2-mm top cover (PMMA) covers the system, resulting in a 10.45-μm-thick cartridge.

Fig. 2 shows the cartridge build-up and demonstrates the fluid flow. When the sample is inserted into the cartridge, it first flows through the shallow flow channel (240-μm thick). Here, the sample makes contact with the deposited MIPs; the small channel ensures a slow flow rate and a long contact time between the MIPs and the sample. Once the sample has flown through the flow channel, it slowly fills up the optical measuring chamber ($\varnothing = 6$ mm). The optical measuring chamber is cut out of thick PMMA (6 mm) ensuring a fluid stack; the measurable color intensity increases when measuring a fluid stack rather than a small flow stream. Once the measuring chamber is filled, a small overflow channel (130-μm-thick tape: 7955MP, 3M, United States) takes over the excess sample. Additional excess fluid is picked up by an array of small capillary pumps ($\varnothing = 1.5$ mm). The total sampled optical path length in the cartridge is equal to 6.37 mm which resembles the combined height of the PET flow channel, optical chamber, and overflow channel. In total, the cartridge can hold 0.85 mL of fluid. However, only 0.40 mL is needed for the fluid to pass the flow channel and fill the optical measuring chamber. The system is closed with a small top cover to make it a closed system wherein a small pressure relief hole is provided to prevent pressure built-up in the system. All parts are stacked together with double-sided adhesive (7955MP, 3M, United States) which provided a watertight seal to the cartridge. All materials (transparent PMMA, PET, and tape) are lasercut to size (Speedy100R, Trotec, Austria). Low-cost prototyping materials and tools were used for ease of manufacturing and to ensure disposability.

B. Spectrometer-on-Chip Sensing Setup

A spectrometer-on-chip sensing setup (Fig. 3) is designed to determine the color intensity of the sample. When the

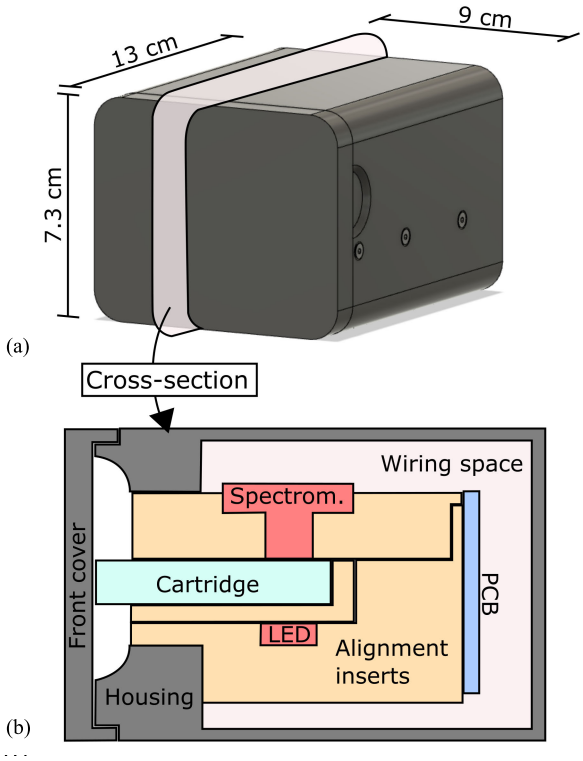

Fig. 3. Spectrometer-on-ship sensing system: (a) enclosed casing that holds all the measuring components and cartridge and (b) schematic cross section of the casing where all relevant parts are indicated.

cartridge is inserted into the measuring setup, the optical measuring chamber of the cartridge ($\varnothing = 6$ mm) is perfectly aligned with a mini-spectrometer (Hamamatsu C12880MA, Japan) positioned at the top, and an LED (HZ-SMD2835W-H, CRI > 97, China) at the bottom, with the spectrometer and the LED being 15.3 mm apart from each other. The spectrometer is sensitive to light wavelengths between 305 and 819 nm, while the LED is only active between 400 and 680 nm. Therefore, in all the following figures, the wavelength range is set at 400–700 nm to visualize the useful range. The LED characteristics are provided in the Appendix. Alignment inserts inside the housing provide a reproducible measuring setup with the correct optical path alignment. The spectrometer and LED are controlled via a microcontroller (ESP32-WROOM-32E-N4) onto a custom PCB. A single USB-C cable makes the connection to a computer. A Python-based dashboard is used to send serial commands and visualize the data in real time. When measuring a spectrum, the LED is set to illuminate while the spectrometer measures the light intensity for 100 μs; this integration time lets in the maximum incident light without saturating the spectrometer. Twenty consecutive measurements are performed, and the average is used to represent a single data point. All spectral analyses are saved in a .csv file for further data processing. Finally, the case is closed with a front cover to avoid any incident light from the outside. The housing and different inserts were 3-D printed (Prusa MINI+, Prusa, Czech Republic; PLA (galaxy black), Prusament, Czech Republic) to size.

Fig. 3(b) shows the cross section of the standard setup for measuring the cartridge with the corresponding alignment inset. However, in addition to measuring the color intensity

inside the cartridge, a specific insert was made that fits standard lab cuvettes (Macro, PS, Brand, Germany). This provides a way to benchmark the performance of the spectrometer-on-chip as it is possible to analyze the exact same samples inside the portable sensing setup as well as inside a high-end lab spectrometer (Nanodrop 2000c, Thermo Fisher, United States). In this configuration, the case is placed on its back cover to measure horizontally through a cuvette as is done in conventional lab-grade spectrometers (Appendix: system in cuvette-measuring mode).

C. MIP Dye Displacement

The dye displacement assay acts as a competitive assay between the target analyte and the loaded dye. In this study, dye-loaded ready-to-use acrylic bulk MIPs were utilized that were synthesized at Maastricht University and imprinted for targeting a designer drug called 2-MXP, as described in previous work [11]. After the removal of the template molecule (2-MXP), the MIPs were loaded with Malachite Green dye. This combination has proven to be successful for the selective detection of diarylethylamines in prior research [11].

D. Measuring Protocol

To exclude the influence of the measurement setup, additional data processing is necessary. First, a measurement is taken using a reference sample. This registered optical behavior is then taken into account to determine the sample's optical characteristics. This ensures that the optical sample properties can be correctly registered during the measurement without any external influence; a comparable process that is also used in conventional spectrometers. The true sample absorbance is calculated according to a calibration trend provided in the datasheet [LOG(Reference intensities/Sample intensities)]. The specific type of used reference sample depends on the nature of the sample under study; these are later specified in Section II-E. However, as it would be impractical for a portable sensing setup to always demand a reference sample, a reference measurement can be saved for later use. Consequently, when analyzing a sample type that has been examined before, the reference values can be requested in software. Additionally, a baseline correction at 710 nm was performed on all spectra obtained from the developed sensor as well as the lab-grade spectrometer. A step-by-step schematic visualizes the working steps in using the cartridge for analysis in the Appendix.

E. Design of Experiments

To assess the sensing setup's capability to analyze dyes with different colors, spectra were recorded for various commercial dyes. Food coloring (Albert Heijn B.V., The Netherlands) was dissolved into ultrapure water (Milli-Q, Arium pro-VF, Germany) to prepare different liquid color samples (yellow, red, and blue). These samples were measured using the developed sensing system in cuvette mode and validated using a commercial lab-grade spectrometer (Nanodrop 2000c). This approach allowed samples to be measured in the same form factor. A cuvette of ultrapure water was used as a reference. Second, a dilution series (7.5, 3.75, 1.875, 0.938, 0.469, 0.234 μg/mL) of Malachite Green (Thermo Scientific, United States) was measured in the cuvette mode using the developed sensing setup, where after the peak absorbance was determined. Additionally, to validate our results, the same samples were analyzed using a lab-grade spectrometer (Nanodrop 2000c) of which the results are provided in the Appendix. A cuvette filled with ultrapure water was used as a reference. These experiments are performed to prove that the sensing setup can reliably measure color intensity. In a final set of experiments, the MIP-integrated lab-on-chip cartridge was put to the test in dye displacement experiments for the detection of 2-MXP. Approximately 15 mg of MIPs (synthesized at Maastricht University as shown by Lowdon et al. [11]) were immobilized in the flow channel. 600 μL of the different target (2-MXP) concentrations (4, 3, 2, 1.5, 1, 0.5, and 0 mg/mL dissolved in ultrapure water) were flushed through the cartridge, whereafter the maximum absorbance was measured. Every concentration was repeated three times. For each measurement, a new cartridge with new MIPs was used. So, to concisely describe it: for each concentration, three different measurements, that is, three distinct cartridges, were used. A cartridge without MIPs filled with ultrapure water was used as a reference. To maintain a continuous flow of the sample inside the cartridge, a removable liquid column ($\varnothing = 8$ mm) was placed above the inlet wherein the entire volume of the sample was inserted. As a result, the hydrostatic pressure progression of the liquid column and the capillary forces inside the cartridge facilitates a passive flow. All measurements were taken 10 min after sample insertion.

III. Results and Discussion

A. Spectral Analysis Validation

To establish that the developed optical setup can accurately register different color spectra, the sensor was put to the test to analyze different colors. Three different colored solutions (yellow, red, and blue) were measured using the mini-spectrometer setup in the cuvette mode and a lab-grade spectrophotometer. The produced spectra are shown in Fig. 4(a) for the Nanodrop 2000c and in Fig. 4(b) for the developed optical setup.

When comparing these produced spectra, it shows that the developed sensing setup can adequately register different colors. Yet, a lab-grade spectrometer can produce spectra with a higher spectral resolution that can result in a more accurate maximum absorbance value. Nonetheless, the spectral resolution of the developed system seems to be more than adequate to provide an overview of the color spectra. Despite this, in Fig. 4(b), a dip in absorbance can be spotted at a wavelength around 420 nm. This anomaly can be explained by the fact that the used LED has a dip in its emitted light spectrum around this region. The LED characteristic can be seen in the Appendix. Therefore, caution should be taken when specifically analyzing a dye with its peak absorbance in this region (below 450 nm). Nonetheless, as our goal is the detection of Malachite Green with a peak absorbance at 620 nm, it did not influence our readings.

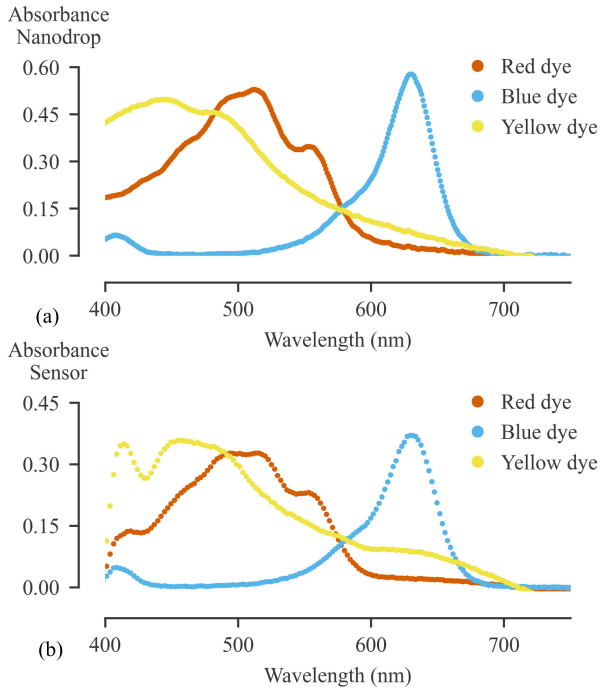

Fig. 4. Spectral comparison of a lab-grade spectrometer to the in-house developed sensing setup. (a) Three different dyes were measured using a lab-grade spectrometer and the spectra are visualized. (b) Likewise, the same samples were measured using our sensing setup.

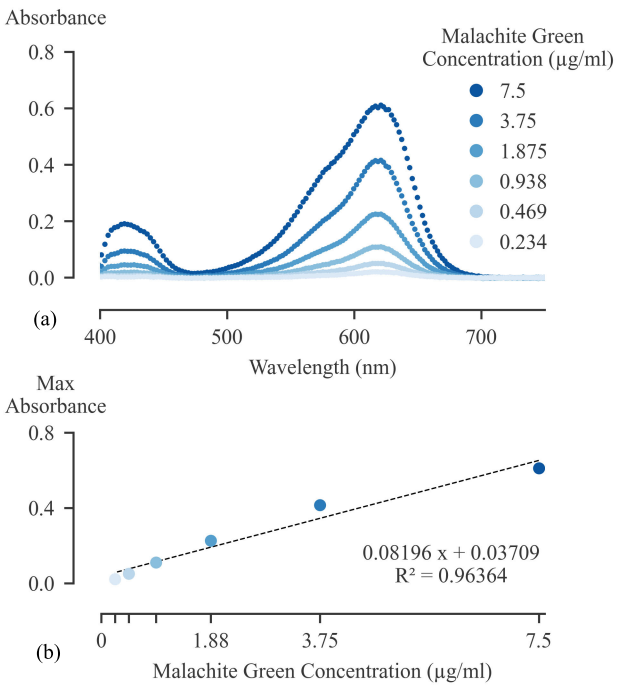

Fig. 5. Spectral analysis of a Malachite Green dilution series. (a) Absorbance spectra as measured using the developed sensing system for various dilutions. (b) Spectral peak absorbance values in function of the Malachite Green concentration. Regression analysis showed a linear relation between the absorbance and Malachite Green concentration (regression values and R^2 values are shown in the figure).

Another difference between the low-cost custom setup and the commercial device is the maximal obtained absorbance values. Overall, for identical samples, the absorbance of the sensor lies slightly below the values obtained by the lab-grade spectrometer. This reasonable discrepancy can be explained by the fact that the cheap developed system cannot achieve the same sensitivity as an expensive lab-grade spectrometer. Furthermore, as this discrepancy can be seen all over the spectra of different samples and colors, there is no indication that this can cause an issue when assessing the relative color intensity. It can, therefore, be concluded that it is possible to use the low-cost developed sensor setup for the spectral analysis of the sample.

B. Spectral Analysis of Malachite Green Dilutions

After the fact is established that the sensor can effectively analyze different colors, the focus lies on the specific detection of Malachite Green. Later on, during the dye displacement experiments, an accurate reading of Malachite Green color intensity is essential to relate the result to an accurate 2-MXP concentration. Therefore, during this experiment, different Malachite Green concentrations were prepared and measured using the cuvette measuring setup.

Fig. 5(a) shows the spectra obtained from analyzing the Malachite Green dilution series. It is clearly evident that as the concentration of Malachite Green increases, the observed absorbance peak at 620 nm also increases. For further processing, the maximum absorbance was calculated between 500 and 700 nm and exported to Fig. 5(b). Fig. 5(b) shows the peak absorbance value according to the Malachite Green concentration. The peak absorbance shows an adequate linear relation to the concentration of Malachite Green. However, due to a fixed detector integration time, a small detector saturation effect is observed at higher concentrations. As a reference, these identical samples (cuvettes) were analyzed using a lab-grade spectrometer with identical data processing (available in the Appendix). Here, great linearity between the maximum absorbance and concentration could be achieved. Yet, high-end spectrometers regulate their integration time to circumvent the detector saturation problem. Additionally, as previously seen in Fig. 4, the maximum absorbance values do not concur. Nevertheless, as both sensing devices show linearity when analyzing the maximum absorbance, no issue is being posed by the discrepancy in absolute maximum values or the slight saturation effect.

Generally, this proves that our sensor can correlate the absorbance to the concentration of Malachite Green. This means that in further experiments, we can rely on the sensor's absorbance reading to linearly assess the presence of Malachite Green in the liquid sample.

C. Lab-on-Chip Cartridge Read-Out for Dye Displacement Analysis

At last, the dye displacement was carried out in the lab-on-chip cartridge and analyzed using the optical sensor setup. Different concentrations (4, 3, 2, 1.5, 1, 0.5, and 0 mg/mL) of 2-MXP were flushed through the cartridge. The dye-displacement MIPs acts as a competitive binding assay; the higher the target concentration in the solution that is flushed through the system, the more dye (Malachite

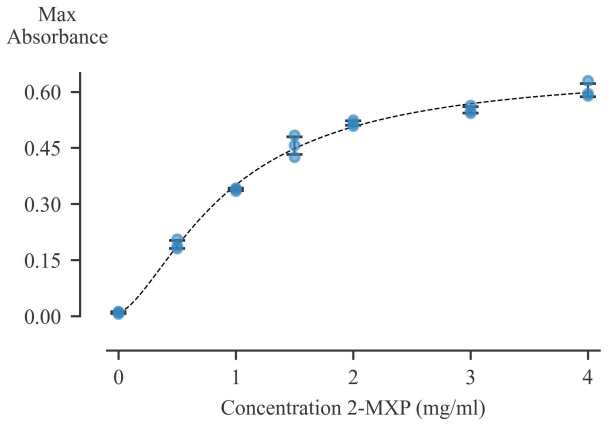

Fig. 6. Measurement of color intensity caused by the MIP dye displacement. Different concentrations of 2-MXP (4, 3, 2, 1.5, 1, 0.5, and 0 mg/mL) were flushed through different cartridges with immobilized MIPs ($n = 7 \times 3$). After dye displacement, the maximum absorbance of the liquid sample was determined. Measurements were performed in triplicate and error bars are shown. A dose–response (4PL) curve is fit.

Green) should be displaced. To determine the performance of the resulting sensor, the absorbance of the liquid inside the cartridge is analyzed after the dye displacement is complete.

Fig. 6 shows the peak absorbance values after flushing different 2-MXP concentrations through the cartridge. Three distinct cartridges were assembled before the addition of the sample in all three. For each concentration, three different measurements, that is, three distinct cartridges, were analyzed whereafter error bars could be plotted. Every measurement was only taken once; no outliers were removed. As expected, the higher the target concentration, the more dye was displaced, and the higher absorbance value was measured. The data were used to construct a dose–response curve that was fit (4PL). A limit of detection (LOD) of 0.070 mg/mL was achieved. The accuracy and precision of the 4PL fit can be seen in Table I. The immobilized MIPs inside the cartridge have a limited amount of binding sites. Therefore, as expected, a saturation occurs where no more dye could be displaced. It should be noted that the optical detector exhibits slight signs of saturation at higher absorbance readings. Thus, the saturation of this curve is primarily caused by the MIP saturation, with a minor contribution from detector saturation. Therefore, the accuracy and precision decrease at higher concentrations. Nevertheless, a high accuracy can be seen when measuring the lower concentration region which for rapid analyte testing seems more than adequate.

During these measurements, the variance between repeats was kept at a minimum. Laser cutting was used to fabricate low-cost material parts which ensured reproducible cartridge assembling. Additionally, the amount of immobilized MIPs mainly depends on the exposed adhesive surface area. Laser cutting was also used to provide cutouts in the adhesive for easy and reproducible powder distribution. Despite these precautions, small deviations in the net MIP weight in between cartridges were unavoidable (14.77 +/− 2.09 mg). However, the experimental data showed no indication that these weight deviations resulted in a significantly different absorbance reading. Based on these observations, the conclusion was drawn

TABLE I
ACCURACY AND PRECISION OF DOSE–RESPONSE (4PL) FIT

Measured Concentration [mg/ml]	*4PL Predicted Concentration [mg/ml]*	*Accuracy [%]*	*Standard Deviation [mg/ml]*
0.0	0.01	/	/
0.5	0.51	2.18	0.02
1.0	0.95	4.59	0.01
1.5	1.56	4.53	0.16
2.0	2.11	5.87	0.07
3.0	2.66	11.19	0.17
4.0	4.67	16.92	1.29

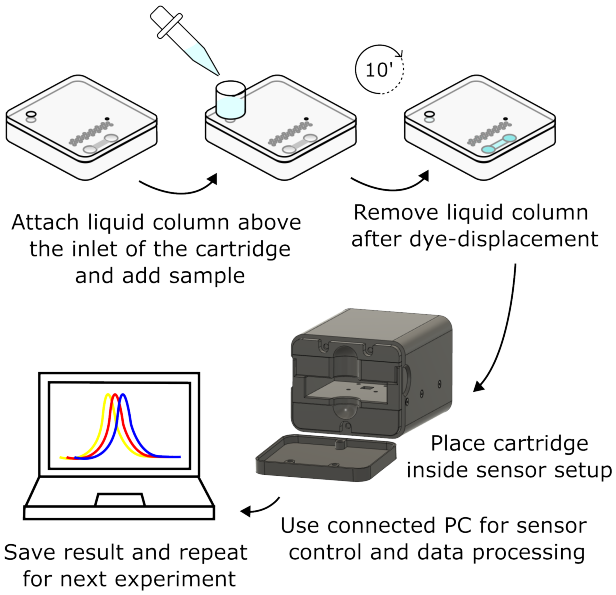

Fig. 7. Flowchart of cartridge handling: The step-by-step schematic visualizes the working steps in using the cartridge for analysis. A liquid column attaches to the cartridge wherein a liquid sample can be inserted. After 10 min, the dye displacement has taken place. Now, the liquid column is removed whereafter the cartridge can be inserted into the optical sensing device. A connected computer is used to control the sensor setup and process the data.

that this method was sufficient to ensure consistent results. At last, the sample flow rate and MIP contact time were kept as consistent as possible. A removable liquid column above the inlet ensured the same hydrostatic pressure progression for the fluid flow. All cartridges were measured 10 min after sample addition.

However, it should be noted that the quality of the dye displacement can highly affect the performance of the measurement setup. Using low-quality MIPs with poor dye displacement efficiency would drastically decrease the accuracy and precision. Nevertheless, these results show that the use of the developed lab-on-chip cartridge in combination with the mini-spectrometer can be an effective way to analyze the dye displacement. Additionally, in the future, improvements could be made to further increase the accuracy of the system by increasing the total sampled optical path length, the total amount of dye loaded, the total contact time to ensure efficient dye displacement, and so on.

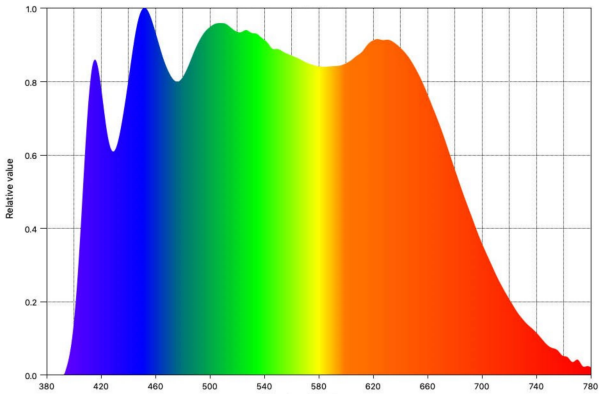

Fig. 8. Excitation spectrum of LED. Specific LED spectrum as provided in the datasheet for HZ-SMD2835W-H. Except for a small dip at 420 and 470 nm, this LED provides an adequately stable emission from 400 to 680 nm.

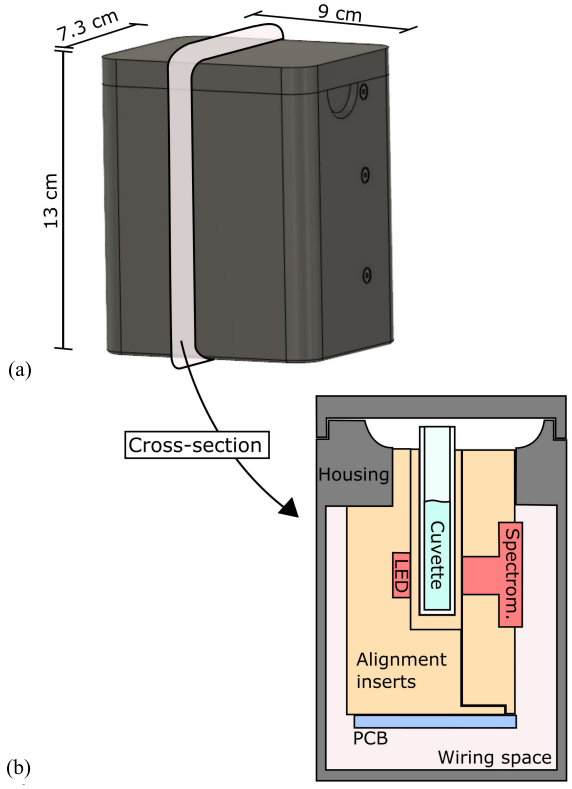

Fig. 9. Spectrometer-on-ship sensing system in the cuvette-measuring mode. (a) Setup is placed on its backside to enable the measurement of standard open lab cuvettes. (b) Schematic cross section of the case where all relevant parts are indicated.

IV. Conclusion

In the presented work, an innovative portable optical sensing setup is presented for rapid analyte testing based on dye-displacement MIPs. Initially, the capability of the sensor to register different colors was established. When comparing the produced spectra to a conventional lab-grade spectrometer, our developed setup proved adequate to visualize color spectra between 400 and 700 nm with a respectable spectral resolution.

Next, different dye dilutions were analyzed. The sensor proved to accurately register the color intensity of different

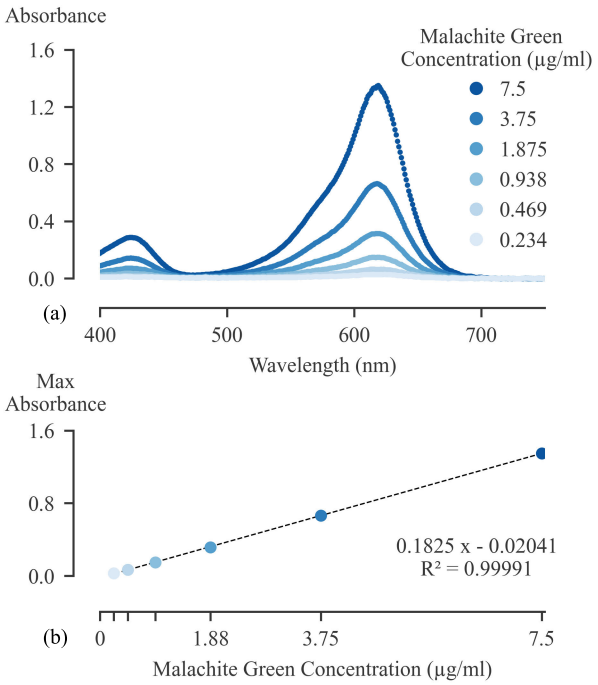

Fig. 10. Spectral analysis of a Malachite Green dilution series. (a) Absorbance spectra as measured using a Nanodrop 2000c for various dilutions. (b) Spectral peak absorbance values in function of the Malachite Green concentration. Regression analysis showed a good linear relation between the absorbance and Malachite Green concentration and validate the findings of our developed sensing system in Fig. 5 (regression values and R^2 values are shown in the figure).

Malachite Green concentrations. The peak absorbance value could be linearly correlated to the dye concentration. These results were validated using a lab-grade spectrometer.

Finally, the use of the optical setup was used to analyze the process of dye displacement. Different analyte (2-MXP) concentrations were flushed through the presented lab-on-chip cartridge and the resulting color intensity (Malachite Green) was analyzed. A dose–response (4PL) curve could successfully be fit on the experimental data. These results proved that the fabrication and assembly process of the cartridge, where the MIP particles are immobilized onto an adhesive, is an easy and effective method for rapid analysis. This can bridge the gap between MIP technology and cost-effective applications.

However, it should be noted that the power of this method extends far beyond the analysis of 2-MXP concentrations. MIP particles are synthetically fabricated for the specific detection of an analyte. This means that these synthetic receptors could also be made for the detection of other analytes for different purposes. To list a few, by synthesizing dye-displacement MIPs targeting other analytes, the measurement setup could also be used for various other applications like assessing food quality, environmental testing, pharmaceutical testing, and so on. This low-cost solution can prove extremely useful for quick on-site or at-line analyte testing.

Appendix

A. Flowchart of the Measurement Protocol

See Fig. 7.

B. LED Characteristic

See Fig. 8.

C. Cuvette Measuring Setup

See Fig. 9.

D. Malachite Green Dilution—Nanodrop

See Fig. 10.

ACKNOWLEDGMENT

The authors would like to thank the staff of UHasselt and Makerspace PXL for their technical support. They would also like to thank Sam Motmans for his contribution to the development of the user interface and preliminary experimental work.

REFERENCES

[1] N. Leibl, K. Haupt, C. Gonzato, and L. Duma, "Molecularly imprinted polymers for chemical sensing: A tutorial review," *Chemosensors*, vol. 9, no. 6, p. 123, May 2021.

[2] M. Cieplak and W. Kutner, "Artificial biosensors: How can molecular imprinting mimic biorecognition?" *Trends Biotechnol.*, vol. 34, no. 11, pp. 922–941, Nov. 2016.

[3] S. Wang, L. Ge, L. Li, M. Yan, S. Ge, and J. Yu, "Molecularly imprinted polymer grafted paper-based multi-disk micro-disk plate for chemiluminescence detection of pesticide," *Biosensors Bioelectron.*, vol. 50, pp. 262–268, Dec. 2013.

[4] N. Cennamo et al., "A novel sensing methodology to detect furfural in water, exploiting MIPs, and inkjet-printed optical waveguides," *IEEE Trans. Instrum. Meas.*, vol. 68, no. 5, pp. 1582–1589, May 2019.

[5] G. De Middeleer, P. Dubruel, and S. De Saeger, "Characterization of MIP and MIP functionalized surfaces: Current state-of-the-art," *Trends Anal. Chem.*, vol. 76, pp. 71–85, Feb. 2016.

[6] H. Zhang, P. Dramou, H. He, S. Tan, C. Pham-Huy, and H. Pan, "Molecularly imprinted stationary phase prepared by reverse microemulsion polymerization for selective recognition of gatifloxacin in aqueous media," *J. Chromatograph. Sci.*, vol. 50, no. 6, pp. 499–508, Jul. 2012.

[7] C. Unger and P. A. Lieberzeit, "Molecularly imprinted thin film surfaces in sensing: Chances and challenges," *Reactive Funct. Polym.*, vol. 161, Apr. 2021, Art. no. 104855.

[8] J. W. Lowdon et al., "MIPs for commercial application in low-cost sensors and assays—An overview of the current status quo," *Sens. Actuators B, Chem.*, vol. 325, Dec. 2020, Art. no. 128973.

[9] C. J. Stephenson and K. D. Shimizu, "Colorimetric and fluorometric molecularly imprinted polymer sensors and binding assays," *Polym. Int.*, vol. 56, no. 4, pp. 482–488, 2007.

[10] J. W. Lowdon et al., "A molecularly imprinted polymer-based dye displacement assay for the rapid visual detection of amphetamine in urine," *Molecules*, vol. 25, no. 22, p. 5222, Nov. 2020.

[11] J. W. Lowdon et al., "Substrate displacement colorimetry for the detection of diarylethylamines," *Sens. Actuators B, Chem.*, vol. 282, pp. 137–144, Mar. 2019.

[12] N. T. Greene and K. D. Shimizu, "Colorimetric molecularly imprinted polymer sensor array using dye displacement," *J. Amer. Chem. Soc.*, vol. 127, no. 15, pp. 5695–5700, Apr. 2005.

[13] Q. Kong, Y. Wang, L. Zhang, S. Ge, and J. Yu, "A novel microfluidic paper-based colorimetric sensor based on molecularly imprinted polymer membranes for highly selective and sensitive detection of bisphenol A," *Sens. Actuators B, Chem.*, vol. 243, pp. 130–136, May 2017.

[14] J. W. Lowdon, H. Diliën, B. van Grinsven, K. Eersels, and T. J. Cleij, "Colorimetric sensing of amoxicillin facilitated by molecularly imprinted polymers," *Polymers*, vol. 13, no. 13, p. 2221, Jul. 2021.

[15] I. O. K'Owino and O. A. Sadik, "Impedance spectroscopy: A powerful tool for rapid biomolecular screening and cell culture monitoring," *Electroanalysis*, vol. 17, no. 23, pp. 2101–2113, Dec. 2005.

[16] S. Abasi, S. Minaei, B. Jamshidi, and D. Fathi, "Development of an optical smart portable instrument for fruit quality detection," *IEEE Trans. Instrum. Meas.*, vol. 70, pp. 1–9, 2021.

[17] C. McVey, C. T. Elliott, A. Cannavan, S. D. Kelly, A. Petchkongkaew, and S. A. Haughey, "Portable spectroscopy for high throughput food authenticity screening: Advancements in technology and integration into digital traceability systems," *Trends Food Sci. Technol.*, vol. 118, pp. 777–790, Dec. 2021.

[18] A. J. Das, A. Wahi, I. Kothari, and R. Raskar, "Ultra-portable, wireless smartphone spectrometer for rapid, non-destructive testing of fruit ripeness," *Sci. Rep.*, vol. 6, no. 1, pp. 1–8, Sep. 2016.

[19] K. Laganovska et al., "Portable low-cost open-source wireless spectrophotometer for fast and reliable measurements," *HardwareX*, vol. 7, Apr. 2020, Art. no. e00108.

[20] S. L. Huey et al., "Portable devices for measurement of vitamin a concentrations in edible oil: Field readiness of available options," *ACS Omega*, vol. 7, no. 21, pp. 17502–17518, May 2022.

[21] N. Chaianantakul et al., "Development of mini-spectrophotometer for determination of plasma glucose," *Spectrochim. Acta A, Mol. Biomol. Spectrosc.*, vol. 204, pp. 670–676, Nov. 2018.

[22] D. González-Morales, A. Valencia, A. Díaz-Nuñez, M. Fuentes-Estrada, O. López-Santos, and O. García-Beltrán, "Development of a low-cost UV-Vis spectrophotometer and its application for the detection of mercuric ions assisted by chemosensors," *Sensors*, vol. 20, no. 3, p. 906, Feb. 2020.

[23] S. Di Nonno and R. Ulber, "Smartphone-based optical analysis systems," *Analyst*, vol. 146, no. 9, pp. 2749–2768, 2021.

[24] I. M. Fermor-Worth and C. Chimerel, "Broadband cavity enhanced UV-VIS absorption spectroscopy for picolitre liquid samples," *Analyst*, vol. 148, no. 8, pp. 1797–1804, 2023.

[25] P. S. Ellis, A. J. Lyddy-Meaney, P. J. Worsfold, and I. D. McKelvie, "Multi-reflection photometric flow cell for use in flow injection analysis of estuarine waters," *Anal. Chim. Acta*, vol. 499, nos. 1–2, pp. 81–89, Dec. 2003.

[26] E. Bodo, V. Bello, V. Asole, and S. Merlo, "Multiwavelength fluidic sensing of water-based solutions in a channel microslide with SWIR LEDs," *IEEE Trans. Instrum. Meas.*, vol. 71, pp. 1–10, 2022.

[27] A. Helander, O. Beck, and M. Bäckberg, "Intoxications by the dissociative new psychoactive substances diphenidine and methoxphenidine," *Clin. Toxicol.*, vol. 53, no. 5, pp. 446–453, May 2015.

[28] D. Luethi, M. C. Hoener, and M. E. Liechti, "Effects of the new psychoactive substances diclofensine, diphenidine, and methoxphenidine on monoaminergic systems," *Eur. J. Pharmacol.*, vol. 819, pp. 242–247, Jan. 2018.

[29] J. W. Lowdon et al., "Surface grafted molecularly imprinted polymeric receptor layers for thermal detection of the new psychoactive substance 2-methoxphenidine," *Sens. Actuators A, Phys.*, vol. 295, pp. 586–595, Aug. 2019.

Juul Goossens received the M.Sc. degree in biomedical sciences with a specialization in bioelectronics and nanotechnology from Hasselt University, Hasselt, Belgium, in 2021, where he is currently pursuing the Ph.D. degree.

He is currently an FWO Fellow with the Biomedical Device Engineering Group, Institute for Materials Research (IMO-IMOMEC), Hasselt University. His current research comprises the development of thermal and impedance sensing technology with a strong focus on biomedical applications. Most recently, his work involved the integration of thermal and impedance sensors into a microplate format, which shows great promise for biological applications.

Thijs Vandenryt received the bachelor's degree in electronics, after an internship, from the Universidade de Vigo, Vigo, Spain, in 2006, and the M.Sc. degree in electrical engineering from XIOS Hogeschool Limburg, Limburg, Belgium, in 2008. He is currently pursuing the Ph.D. degree with Hasselt University, Hasselt, Belgium, with a strong focus on microfluidics and biomedical system integration.

He is currently with the Biomedical Device Engineering Group, Hasselt University, where he is involved in several international projects, designing, and building electronics and microfluidics for sensing applications.

Joseph W. Lowdon received the master's degree in chemistry from Manchester Metropolitan University, Manchester, U.K., in 2017, and the Ph.D. degree in the development of molecularly imprinted polymers (MIPs) toward sensor applications from Maastricht University, Maastricht, The Netherlands, in 2021.

He is currently working as a Post-Doctoral Research with the Sensor Engineering Department, Maastricht University, also working toward the development of sensors toward the detection of small molecules. His research interests include the synthesis of biomimetic polymers for biological and chemical sensing, the synthesis of novel monomers, and conjugated polymers, and the implementation of new sensing technologies targeted toward healthcare management and environmental monitoring.

Bart van Grinsven received the master's degree in bioelectronics and nanotechnology from Hasselt University, Diepenbeek, Belgium, in 2007, and the Ph.D. degree from the Biosensor Group, Hasselt University, in July 2012, promoted by Prof. Dr. Patrick Wagner and Prof. Dr. Michael Schöning.

Then he was employed by TNO as a Development Engineer. After working as a Post-Doctoral Researcher with the Biosensor Group, he then switched to Maastricht University, Maastricht, The Netherlands, where he currently holds the position of Associate Professor and the Group Leader of the Sensor Engineering Department.

Kasper Eersels received the M.Sc. degree in bioelectronics and nanotechnology from Hasselt University, Diepenbeek, Belgium, in 2009, and the Ph.D. degree from Hasselt University.

He is currently an Associate Professor with Maastricht University, Maastricht, The Netherlands, where he works with the Sensor Engineering Department of the Faculty of Science and Engineering on the development of novel biosensor solutions for application in various fields including medical diagnostics, food safety, and environmental screening.

Wim Deferme received the Engineering degree in applied physics from the Technical University of Eindhoven, Eindhoven, The Netherlands, in 2003, and the Ph.D. degree in materials physics from Hasselt University, Diepenbeek, Belgium, in 2009.

In 2009 as a Post-Doctoral, he started research in the field of printable electronics. Since February 2014, he is currently a Professor with Hasselt University heading a group of one Post-Doctoral, seven Ph.D. Students, one full-time Researcher and several bachelor and master's students in the field of "Functional Materials Engineering" focused on printing and coating technology. In the laboratory of inkjet printing, screen printing and ultrasonic spray coating are applied for the deposition of functional inks on substrates such as glass, foils, paper, textiles, and even 3-D objects. Applications focus on organic light-emitting devices, smart sensors for wound monitoring, and stretchable electronics.

Ronald Thoelen received the master's degree in applied physics from TU Eindhoven, Eindhoven, The Netherlands, in 2004, and the Ph.D. degree in physics from Hasselt University, Diepenbeek, Belgium, in 2008 with a focus on impedance-based biosensors.

He has been a Professor with the Faculty of Engineering Technology, Hasselt University, since 2013, and became the Dean of this Faculty in 2022. He is also the Leader of the "Biomedical Device Engineering" Research Group with IMO-IMOMEC, a collaboration between Hasselt University and IMEC. The group focuses on developing specialized sensor devices in the environmental, food, and healthcare industries, with an emphasis on innovations in thermal, electrical, and optical sensor read-out techniques.